Desalination 566 (2023) 116875

Contents lists available at ScienceDirect

Desalination

journal homepage: www.elsevier.com/locate/desal

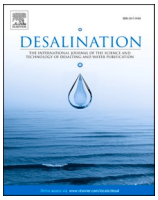

Desalination by batch reverse osmosis (RO) of brackish groundwater containing sparingly soluble salts

Ebrahim Hosseinipour [a], Ellie Harris [a], Hossam A. El Nazer [b], Yasser M.A. Mohamed [b], Philip A. Davies [a,*]

[a] School of Engineering, University of Birmingham, Edgbaston, Birmingham B15 2TT, UK
[b] Photochemistry Department, National Research Centre, P.O. 12622, Egypt

HIGHLIGHTS

- Batch RO successfully treated brackish groundwater at high recovery (80 %) and with low energy consumption (SEC < 0.5 kWh/m^3).
- Despite a high risk of scaling in the simulated groundwater (LSI of 1.7–2.6) no scaling was observed.
- Four anti-scaling mechanisms: periodic flushing, feed flow reversal, osmotic backwash, and salinity cycling
- SEC was comparable (within 7 %) to that of batch RO treating pure NaCl solutions

GRAPHICAL ABSTRACT

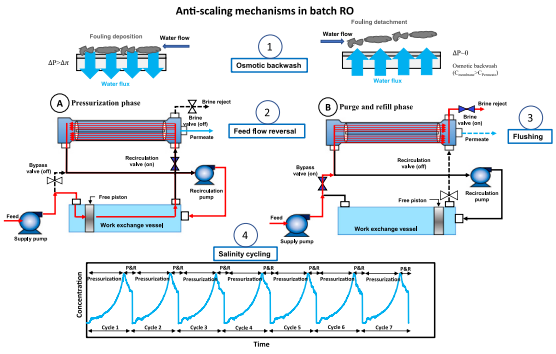

ARTICLE INFO

Keywords:
Scaling
Osmotic backwash
Periodic flushing
Feed flow reversal
Salinity cycling

ABSTRACT

Batch RO desalination is a new approach to high-recovery, energy-efficient desalination. So far, however, batch RO has been tested mostly with pure sodium chloride solutions. An important application of batch RO is desalination of brackish groundwater which, besides sodium chloride, contains sparingly soluble salts. In this experimental study of a batch RO system, we used simulated groundwater (with total dissolved solids ranging from 1180 to 3637 mg/L) following compositions of samples taken from a location in Egypt and a location in India. The groundwater contained high levels of salts which could be expected to cause scaling on the RO membrane surface. For example, the Langelier Saturation Index (*LSI*) for calcite reached 2.6 in the brine. Nonetheless, the system resisted scaling throughout >100 h of operation. Membrane permeability remained almost unchanged, as demonstrated by tests conducted before and after the experiments. Induction time calculations showed that salinity cycling did not fully explain the scaling inhibition. Other anti-scaling mechanisms – such as periodic flushing, osmotic backwash, and feed flow reversal – were also likely contributors. At recovery of 0.8, hydraulic specific energy consumption (*SEC*) was <0.5 kWh/m^3 and close to that obtained with sodium chloride solution at equivalent osmotic pressure.

* Corresponding author.
E-mail address: p.a.davies@bham.ac.uk (P.A. Davies).

https://doi.org/10.1016/j.desal.2023.116875
Received 18 May 2023; Received in revised form 21 July 2023; Accepted 25 July 2023
Available online 28 July 2023

1. Introduction

Batch RO is a relatively new approach to desalination that has gained interest because it achieves high efficiency and recovery rates in a compact design [1]. However, much of the research on batch RO has been done with feed water containing a solution of a single salt – typically sodium chloride (NaCl). For example, using NaCl solution, Wei et al. [2] studied a batch RO system to conclude that (compared to standard continuous RO) batch RO could save about 11 % of energy in the desalination of seawater at recovery of 0.55. In a study of brackish water desalination, Hosseinipour et al. [3] measured the performance of a batch RO system, fed by NaCl solution of concentration 1000–5000 mg/L and obtained electrical *SEC* of 0.48–0.83 kWh/m^3 at a recovery of 0.8. This was better than achieved by most existing brackish RO systems. Compared to standard RO, batch RO allows recovery to increase without large penalties in *SEC*. Thus, by operating in hybrid semi-batch/batch mode, batch RO achieved recovery of 0.94 with *SEC* of just 0.54 kWh/m^3 using NaCl feed solution of concentration 1500 mg/L [1].

Though these studies have shown batch RO to be a promising technology, for practical applications it is important to understand how it will perform with realistic feed water compositions containing multiple components as opposed to simple NaCl solution. One important category of feed water is brackish groundwater which occurs in many aquifers exploited by humans across the world. Brackish water desalination accounts for about 25 % of the RO desalination output globally [4]. Typically, brackish groundwater contains many other salts besides sodium chloride, dependent on the geology of the aquifer from which it is extracted [5]. Because of its high energy efficiency at high recovery, batch RO is envisaged as a good solution to desalinate groundwater. However, given the many and varied groundwater compositions occurring worldwide, testing batch RO with every possible composition is not practical. Therefore, if experiments and models based on sodium chloride are a good representation of performance with more complex compositions, this will be a very useful simplification when it comes to developing and testing batch RO technology.

Unlike sodium chloride, some of the other salts in groundwater may be sparingly soluble. Such salts are prone to precipitate on the membrane surface, thus causing mineral fouling (i.e., scaling) which can lead to loss of performance, manifested as decreased permeate output or increased pumping pressure and energy consumption. Sparingly soluble salts common in groundwater include $CaCO_3$, $CaSO_4$, $BaSO_4$, $SrSO_4$, CaF_2, and $Ca_3(PO_4)_2$. According to Liu et al. [6], calcium carbonate ($CaCO_3$) and calcium sulfate ($CaSO_4$) are the most prevalent sources of scaling in RO desalination. To mitigate scaling, acid [7] and anti-scalants [8–10] are often dosed to the feed of groundwater RO plants. The required dosing volume depends highly on the recovery of the plant which is constrained by the presence of the sparingly soluble salts. Thus, to reduce the usage, cost, and environmental impact of the anti-scalant chemicals, designers may prefer to decrease the plant's recovery in some cases [11]. Even with anti-scalant dosing, Ruiz-Garcia et al. [12] reported a limitation in recovery to a maximum of 0.76 using Genesys anti-scalants, depending on the feed composition of the brackish water source. In contrast to such need to limit recovery, the cost-efficient operation of inland brackish water RO favours high recovery [12–14].

The cyclic nature of the batch RO process provides four mechanisms that could provide advantages over standard continuous RO when it comes to avoiding fouling and scaling at high recovery. Each mechanism has been used individually in other RO or other membrane separation processes, but all four are brought together in batch RO [15].

The first mechanism is flushing, which occurs towards the end of each cycle of the batch RO operation. During the initial phase of the cycle (i.e., pressurisation) the concentration in the RO channel gradually increases above the feed concentration. Precipitation and scaling by salts could be expected at these elevated concentrations. Then, during subsequent flushing, the concentration falls back down close to the feed concentration – providing an opportunity to redissolve any precipitated salts and remove them from the membrane surface. Permeate output flow is paused such that precipitates are no longer drawn towards the membrane; while tangential flow continues and provides a cleaning action to sweep away deposits. Flushing is already a common method to remove scaling and fouling in many types of membrane processes. It is regularly used, for example, in clean-in-place procedures in standard RO plants [16]. In batch RO, however, the role of flushing is less well known and understood.

The second mechanism is osmotic backwash, which occurs at the end of the pressurisation phase of each batch RO cycle. At this moment, the feed pressure falls suddenly, such that the osmotic pressure of the brine causes permeate to flow back through the membrane and into the feed channel [2]. This backflow continues until enough flushing has taken place to lower the osmotic pressure in the feed channel. Osmotic backwash has a downside in that it reduces output and recovery slightly, but the upside is that it may help to restore membrane permeability by lifting scaling species off the membrane. Many studies have confirmed the foulant removal potential and flux restoration of cleaning RO membranes using the osmotic backwash method [17–23]. For example, in a UF-RO pilot system treating secondary treated effluent, a direct osmosis backwash using high-salinity solution injection (varying from 100 to 136 g/L) was studied [17]. The study reported a five-fold increase in brine turbidity (3 NTU) compared to the normal process without osmotic backwash (0.6 NTU), showing that foulants were effectively removed and carried away in the brine stream. Osmotic backwash is not unique to batch RO, as it can occur in other types of RO where permeate flow is intermittent. For example, battery-less solar-powered RO systems experience starting and stopping of permeate production as solar radiation varies over the diurnal cycle or more frequently [24]. Even grid-connected continuous RO systems could be controlled to provide osmotic backwash through deliberate stopping and starting. Nevertheless, the periodic and frequent (i.e., every few minutes) occurrences of osmotic backwash in batch RO make it particularly relevant for this technology.

Thirdly, feed flow reversal occurs in some batch RO systems, which can also be beneficial to delay nucleation and thus counter scaling. In a standard continuous RO system, scaling normally begins near the brine outlet end of the RO module, where the concentration of minerals is highest [25,26]. Feed flow reversal could mitigate scaling by periodically introducing fresh feed at the outlet (i.e., by swapping the inlet and outlet), thus disrupting precipitation and preventing or redissolving scale before it builds up significantly. Again, this is not unique to batch RO. Feed flow reversal RO exists as a non-batch RO technology designed to take advantage of this effect and reduce anti-scalant dosage [27,28]. In 2012, for example, Gu et al. [29] demonstrated feed flow reversal at recovery up to 0.81 without anti-scalant, despite calcium sulfate (gypsum) saturation index reaching 0.54 at the RO outlet. Batch RO may provide varying degrees of feed flow reversal, depending on the configuration chosen. For example, double-acting batch RO systems can provide full flow reversal, meaning that equal operation time is spent running in either flow direction [30,31]. Some single-acting batch RO systems use no feed flow reversal; whereas others use partial feed flow reversal, meaning that flow is reversed for a shorter period corresponding to the purge phase of operation only [32] – as is the case in the current study.

Fourthly, salinity cycling in batch RO may also help reduce scaling. Although, for a given recovery, the final concentration in batch RO must reach the same maximum as in continuous RO, the maximum is only reached momentarily during the batch RO cycle. Supersaturated conditions are therefore only transient, such that scaling may be avoided if they do not persist sufficiently for salt crystals to nucleate [33,34]. In a study of salinity cycling, Warsinger et al. [33] used a model of crystal nucleation to predict promising anti-scaling performance of batch or semi-batch RO processes treating $CaCO_3$ and $CaSO_4$ solutions. The study used the following correlation between the nucleation induction time and saturation index of $CaCO_3$ which crystalises as calcite:

$$t_{ind,CaCO_3} = 10^{\left(4.22-\frac{13.8}{LSI}-\frac{1876.4}{T}+\frac{6259.6}{LSI\,T}\right)} \quad (1)$$

where $t_{ind,CaCO_3}$ is the nucleation induction time [s], *LSI* is the Langelier saturation index, and T is the absolute temperature [K]. For $CaSO_4$, which crystallises as gypsum, the following correlation was used [33]:

$$t_{ind,CaSO_4} = 55.5\ SI^{-4.701} \qquad SI < 0.2 \quad (2)$$

where *SI* is the saturation index. By comparing the residence time of the water to the nucleation induction times calculated, the study predicted the scaling of the salts based on residence times in typical RO systems and predicted the maximum possible recovery for batch vs. standard continuous RO, assuming saturated feed solutions. In the case of $CaCO_3$, it predicted significant bulk nucleation starting at recovery $r = 0.87$ in batch RO, compared to only $r = 0.74$ in standard continuous RO [33]. In the case of $CaSO_4$, the corresponding thresholds were $r = 0.87$ (batch) vs $r = 0.54$ (continuous). Thus, batch RO should be able to operate at $r = 0.87$ when challenged with either of these sparingly soluble salts. This is a high recovery compared to many current groundwater desalination systems.

To investigate the hypothesis that batch RO helps to reduce fouling, this paper reports laboratory experiments with a single-acting batch RO system that includes these four features of periodic flushing, osmotic backwash, feed flow reversal, and salinity cycling. Unlike most previous experimental studies which used only sodium chloride, the experiments have been performed with feedwater which poses a risk of mineral scaling. The feedwater was made up to replicate samples taken in the field in two case study locations, one in Egypt and the other in India. In both cases, groundwater quality is poor, and desalination is required to upgrade it for drinking and irrigation purposes. Therefore, the use of batch RO is of practical interest to address the scarcity of good-quality water in both locations. Using these groundwater compositions, this paper quantifies important performance parameters, including *SEC*, peak pressure and rejection and compares these to the experimental and modeling results obtained previously with sodium chloride. By testing performance before and after the series of tests, we show that no significant drop in performance occurred. The Discussion section analyses the results in comparison to other studies that used similar approaches to avoid scaling in various types of RO system.

2. Case study locations

2.1. Siwa Oasis, Egypt

The first location is Siwa Oasis, Egypt, where samples have been taken from the Tertiary Carbonate Aquifer System. This is a shallow limestone aquifer, of depth 10–200 m, characterized by its medium to high salinity: the samples contained total dissolved solids (TDS) of 1300–8600 mg/L (with an average of 4200 mg/L). Siwa Oasis is considered among the most promising locations in the Western Desert of Egypt for future agricultural expansion projects because of the availability of groundwater. Currently, the aquifer is exploited mainly for the irrigation of crops such as dates and olives. The use of irrigation, together with the high rate of evaporation during the summer, leads to the development of a thick salty layer that hampers such agricultural activities [35]. The uncontrolled withdrawal of groundwater and agricultural expansion in the last decades has led to the decline of piezometric head levels and the deterioration of groundwater quality [36]. Consequently, Siwa Oasis suffers from environmental problems including water logging, soil salinization, inefficiency of disposed drainage water systems, and loss of agricultural productivity. As a result of the increased salinity in the groundwater wells, it has been suggested to construct RO desalination systems to enhance the water quality for irrigation [37]. Nonetheless, the presence of limestone in the aquifer is likely to present a challenge for RO because of calcite scaling.

2.2. Saurashtra region, Gujarat, India

The second location is the semi-arid Saurashtra region of the Indian state of Gujarat, where the coastal strip has become severely affected by saline intrusion. A recent field study focused on Lodhva, a village of about 8500 inhabitants that has relied on groundwater for domestic, agricultural, and industrial uses [38]. There are limestone reserves in this area, and numerous cement businesses engage in open-pit mining. The coastal aquifer has been made is more susceptible to seawater intrusion by such mining. Deterioration in groundwater quality, which now typically contains 2000–3500 mg/L of dissolved solids, effectively renders it unfit for human consumption. Consequently, piped water has been introduced to provide drinking water from distant reservoirs. Nevertheless, the supply of such water is intermittent and not accessible to all villagers; and its quality cannot be guaranteed. As regards the disposal of wastewater, Lodhva has no infrastructure or treatment systems for this purpose. Domestic wastewater is mostly discharged to simple soak pits adjacent to buildings. The problems at Lodhva are typical of those in Saurashtra and more broadly across Gujarat – which has over 3500 km^2 of salinized land in total [38].

3. Materials and methods

3.1. Feedwater composition

The feedwater compositions used in this study are based on the analysis of field samples from the above two locations, as reported in [37,38]. In total, 54 sample compositions were reported from Siwa (Egypt) and 20 from Lodhva (India) – henceforth referred to simply as Egypt (E) and India (I) samples, respectively. Each sample was taken from a different well. Four sample compositions have been chosen from each location, giving eight in total. The TDS of the chosen compositions ranged from 1138 to 3492 mg/L (see Table A1). These compositions represent a range of salinities at each location (though some higher salinities had to be excluded because of the 25-bar pressure limit of the batch RO equipment used in this study). At these TDS levels, none of these compositions meets general water quality requirements for drinking. The levels would also exceed the acceptable limits of many irrigated crops.

A Piper diagram has been used to classify groundwater quality (Fig. 1). In the cation plot (left triangle), the Egypt samples lie towards the alkali metal ($Na^+ + K^+$) vertex, indicating the dominance of these cations. The India samples lie more towards the Ca^{2+} vertex, showing a greater abundance of calcium, which may be problematic for scaling. In the anion plot (right triangle), all samples fall close to the halide ($Cl^- + F^-$) vertex. The diamond plot shows that the Egypt samples are dominant in (Na^+– K^+– Cl^-–SO_4^{2-} type) indicating the prevalence of alkali metal ions ($Na^+ + K^+$) and stronger acidic anions ($Cl^- + SO_4^{2-}$) over the alkaline earth ($Ca^{2+} + Mg^{2+}$) and weaker acidic anions ($CO_3^{2-} + HCO_3^-$). The India samples are dominated by cations (Ca^{2+} and Mg^{2+}) and anions (SO_4^{2-} and Cl^-), which indicates permanent hardness in the water (Ca^{2+}-Mg^{2+}-Cl^--SO_4^{2-} type). The Na/Cl ratio indicates that all the India samples (I1-I4) have a ratio of <0.86, confirming that the wells are affected by seawater intrusion.

The compositions were checked for charge neutrality (ignoring minor ions at concentrations <1 mg/L). The discrepancy in the Egypt samples was <0.4 %; whereas in the India samples it was as high as 6 and 9 % in the case of samples I1 and I2, respectively (that of I3 and I4 was <1 %). Adjustments to charge balance were therefore necessary before making up the feedwater. The adjustments were made preferentially to the higher concentrations of ions present to follow the reported compositions as closely as possible. For example, Table 1 shows the adjustments for sample E2. The total amount of cations reported was $\sum C^{Z+} = 30470\ \mu eq/L$, while the total amount of anions was $\sum A^{Z-} = 30310\ \mu eq/L$. Therefore, we balanced them to the average value of $\sum$

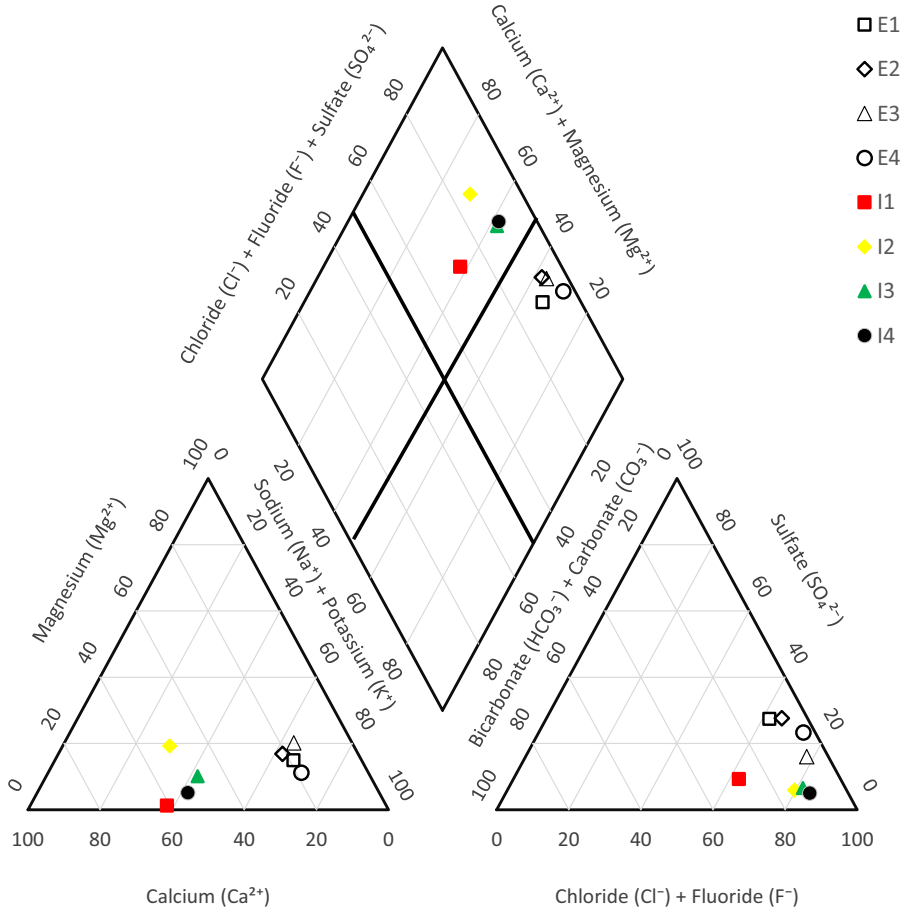

Fig. 1. Piper diagram for groundwater quality in Egypt (E1-E4) and India (I1-I4).

Table 1
Charge balance adjustments for sample E2 (see Appendix for similar details for other samples).

Ions	Measured value (mg/L)	Measured value (μeq/L)	Adjustments (μeq/L)	Balanced concentration (μeq/L)	Balanced concentration (mg/L)
Ca^{2+}	128	6384	−17	6367	127.7
Mg^{2+}	62.4	5136	−13	5122	62.2
Na^{+}	423.2	18,408	−48	18,360	422.1
K^{+}	20.28	519	−1	517	20.2
NH_4^{+}	0.42	23	0	23	0.4
$\sum C^{z+}$	–	30,470	−80	30,390	–
HCO_3^{-}	131.76	2160	6	2166	132.1
Cl^{-}	700	19,774	52	19,826	701.8
SO_4^{2-}	401.28	8351	22	8373	402.3
NO_3^{-}	1.51	24	0	24	1.5
$\sum A^{z-}$	–	30,310	80	30,390	–

Table 2
Ionic composition of feed water used in the experiments, following adjustment of change balance. The pH was measured after making up the tanks, without any adjustment.

	Sample number	pH	TDS (mg/L)	Ca^{2+} (mg/L)	Mg^{2+} (mg/L)	Na^{+} (mg/L)	K^{+} (mg/L)	NH_4^{+} (mg/L)	HCO_3^{-} (mg/L)	Cl^{-} (mg/L)	SO_4^{2-} (mg/L)	NO_3^{-} (mg/L)	F^{-} (mg/L)
Egypt	E1	7.8	1319	79.6	38.2	315.1	9.3	0.3	136.6	462	276.5	0.8	–
	E2	7.9	1871	127.7	62.2	422.1	20.2	0.4	132.1	701.8	402.3	1.5	–
	E3	7.9	2788	151.5	114.8	669.7	25.8	0.6	171.3	1292	359.3	2.1	–
	E4	7.9	3637	223.2	81.3	951.7	28.3	0.7	120	1560	669	1.9	–
India	I1	7.9	1180	217.4	2.7	153	4.4	–	278.2	364.1	72.9	85.5	0.6
	I2	7.9	1994	338.1	77.4	222.4	5.6	–	277.2	885.5	89	96.2	0.6
	13	7.9	2576	411.8	52.7	407.8	11	–	305.4	1226	133	26	0.6
	I4	7.9	2811	507.1	15	439.2	32	–	296.3	1360	109.8	50.5	0.6

$C^{Z+} = \sum A^{Z-} = 30390$ mainly by adjusting the concentrations of Na^+ and Cl^- which were the most concentrated ions in this case. Table 2 shows the ionic compositions used for the experiments, following similar adjustments in each of the 8 cases.

The scaling potential of these compositions was analysed with the help of PHREEQC software [39] applied to the feed and brine composition. The brine composition was based on a recovery of $r = 0.8$, corresponding to a fivefold increase in the concentration of all species with respect to the feed. By calculating the saturation indices of the various salts, PHREECQ identified three species at risk of scaling: $CaCO_3$, $CaSO_4$ and CaF_2. In the case of CaF_2, we took into account the background concentration of 0.6 mg/L fluoride ions in the tap water used to prepare the feed water. This was significant as the solubility of CaF_2 is only 15 mg/L at 25 °C, such that the addition of just small amounts of fluoride can affect saturation. For $CaCO_3$, solubility is pH-dependent, and the Langelier Saturation Index (*LSI*) is used instead of the simple saturation index (*SI*). A value of *LSI* or *SI* greater than zero indicates supersaturation of the respective salt and thus a risk of scaling [40].

As seen in Table 3, all brine compositions had a high calcium carbonate scaling potential ($LSI > 0$ with values up to 2.6) which may cause calcite to precipitate on the membrane. For comparison, Ruiz-Garcia et al. [12] found that, even using anti-scalants, the maximum allowable LSI was in the range of 2.4 to 3 and this placed an important limitation on the recovery achievable in their standard RO system. The *LSI* values of the India compositions were much higher than those of the Egypt compositions, sometimes exceeding 0 in the feed and not only the brine. Calcium fluoride was also saturated in the brine, especially in the India compositions. In contrast, there is little risk of calcium sulfate scaling because the corresponding *SI* is negative except for a small positive value in the brine for E4.

Overall, the brine has a high scaling potential. Scaling could be expected to occur towards the outlet of an RO module in standard, continuous flow RO desalination. Anti-scalant chemicals would normally be used in such applications. According to proprietary software, dosing of 2 mg of anti-scalant per L of feedwater would be recommended in all eight cases. This confirms that these are suitable compositions to evaluate batch RO for the possible occurrence of scaling.

3.2. Feedwater preparation

The method of Smith et al. [41] was used to formulate and prepare the feed water solutions. Low solubility salts such as calcium sulfate and magnesium carbonate were avoided since they are difficult to dissolve and may precipitate (for example, Table 4 shows low solubility salts avoided in the case E2). We grouped the required salts in compatible combinations into the minimum number of stock solutions. Thus, Table 5 shows the eight recipes used for feedwater preparation.

All chemicals were of analytical grade (purity >99 %) and purchased from Sigma-Aldrich. The recipes were used to make up the feed tank volume of 1200 L for each test, using tap water with TDS <100 mg/L. To ensure dissolution and mixing, each salt was mixed with hot tap water (at 50–60 °C) in smaller volumes before being added to the main feed tank. Once all salts had been added, the feed tank was topped up to a final volume of 1200 L as indicated by a weighing scale underneath the tank (accuracy of ±0.2 kg). Using a recirculating pump, the feed solution in the tank was further mixed for about an hour before the start of each experiment. At the same time, using submersible titanium heaters (D-D Premium Aqua Supply GmbH) and a thermostat, the temperature was raised to 25 ± 0.1 °C and then kept constant during the experiments.

Table 4
Matrix of the salts used for the preparation of composition E2 using the balanced concentrations calculated in Table 1 (see Appendix for similar data for other samples). The red highlighted cells indicate possible salt combinations that would result in insoluble salts and were therefore avoided.

Ions	HCO_3^- (μeq/L)	Cl^- (μeq/L)	SO_4^{2-} (μeq/L)	NO_3^- (μeq/L)	$\sum C^{Z+}$
Ca^{2+} (μeq/L)		6367		_	6367
Mg^{2+} (μeq/L)		_	5122	_	5122
Na^+ (μeq/L)	1673	13436	3251	_	18360
K^+ (μeq/L)	493	_	_	24	517
NH_4^+ (μeq/L)		23	_		23
$\sum A^{Z-}$	2166	19826	8373	24	_

3.3. Experimental equipment and procedure

The batch RO laboratory equipment used a single-acting free piston design (see Fig. 2). A description of the equipment and experimental procedure, as used previously to treat NaCl solution, has already been provided [3] and is not therefore repeated here. Based on the earlier findings, a ratio of recirculation flow to feed flow of $Q_{recirc}/Q_{feed} \sim 2$ was chosen to minimize *SEC*. Like in [3], the membrane used was a Dupont Eco Pro-440, 8-in. module with an active membrane area of 41 m^2. The flux varied from 11 to 23 L/m^2/h (corresponding to feed flow rates of about 8.4 to 16.4 L/min), giving an output of about 10 to 17 m^3/day. The system was operated at the design recovery of $r = 0.8$.

As reported in [3], salt retention causes an increase in concentration during the initial cycles. The system reaches a stable condition after 3–4 cycles. Therefore, the recorded data of the fourth cycle (including changes in the weight of the tanks, conductivities, pressures, flow rates, and power consumption of the two feed and recirculation pumps) was

Table 3
Scaling potential of calcium carbonate (as calcite), calcium sulfate (as gypsum), and calcium fluoride (as fluorite) in different feed compositions (by PHREEQC software) at 25 °C. Saturation index $SI_y = \log (IAP_y/KP_{sp,y})$, where IAP_y and $KP_{sp,y}$ are the ion activity and solubility products of mineral scalant y, respectively.

Origin	Composition	Langelier Saturation Index, *LSI* ($CaCO_3$)		Saturation Index			
				SI ($CaSO_4{\cdot}2H_2O$)		*SI* (CaF_2)	
		Feed	Brine	Feed	Brine	Feed	Brine
Siwa Oasis, Egypt	E1	0.35	1.66	−1.23	−0.31	−1.54	0.21
	E2	0.46	1.79	−1.01	−0.1	−1.45	0.32
	E3	0.69	1.88	−1.09	−0.21	−1.48	0.33
	E4	0.63	1.81	−0.74	0.11	−1.35	0.45
Gujarat, India	I1	1.15	2.42	−1.35	−0.39	−0.83	0.87
	I2	1.25	2.47	−1.28	−0.34	−0.82	0.94
	I3	1.35	2.55	−1.09	−0.19	−0.75	0.99
	I4	1.41	2.6	−1.08	−0.19	−0.64	1.07

Table 5
Recipes for preparation of the feed water compositions representative of Egypt (E1-E4) and India (I1-I4) groundwater samples.

Required salts	Concentration															
	E1		E2		E3		E4		I1		I2		I3		I4	
	μeq/L	mg/L	μeq/L	mg/L	μeq/L	mg/L	μeq/L	mg/L	μeq/L	mg/L	μeq/L	mg/L	μeq/L	mg/L	μeq/L	mg/L
$CaCl_2$	3979	441.6	6367	706.6	7557	838.7	11,132	1235.4	10,306	1143.8	16,848	1869.8	20,524	2277.8	25,280	2805.6
$MgSO_4$	3152	379.4	5122	616.5	–	–	6692	805.5	219	26.4	1854	223.2	2771	333.5	–	–
NaCl	8866	518.1	13,436	785.2	19,458	1137.1	32,886	1921.9	–	–	3678	214.9	12,554	733.7	11,947	698.2
$NaHCO_3$	2246	188.7	1673	140.5	2183	183.4	1273	106.9	4559	434	4545	381.8	5006	420.6	4858	408.1
Na_2SO_4	2617	371.7	3251	461.8	7480	1062.5	7231	1027.1	1213	172.3	–	–	–	–	2285	324.6
$KHCO_3$	–	–	493	49.4	626	62.7	694	69.5	–	–	–	–	–	–	–	–
NH_4Cl	14	0.75	23	1.2	33	1.8	37	2	–	–	–	–	–	–	–	–
KNO_3	12	1.2	24	2.4	34	3.4	30	3	–	–	109	11	–	–	789	79.8
KCl	227	16.9	–	–	–	–	–	–	–	–	–	–	–	–	–	–
$MgCl_2$	–	–	–	–	9452	899.9	–	–	–	–	4511	429.5	1569	149.4	1195	113.8
$NaNO_3$	–	–	–	–	–	–	–	–	871	74	1445	122.8	166	14.1	118	10
K_3PO_4	–	–	–	–	–	–	–	–	17	3.6	23	4.9	16	3.4	18	3.8
K_2SO_4	–	–	–	–	–	–	–	–	86	15	–	–	–	–	–	–
$Ca(NO_3)_2$	–	–	–	–	–	–	–	–	512	84	–	–	–	–	–	–
$Mg(NO_3)_2$	–	–	–	–	–	–	–	–	–	–	–	–	–	–	26	3.9
KF	–	–	–	–	–	–	–	–	10	0.6	10	0.6	11	0.65	10	0.6

used for the calculation of the results. This corresponded to a total duration of 330 to 580 s for each cycle (including a purge-and-refill phase of about 75 s), with shorter durations corresponding to higher water fluxes. Therefore, the total duration of each run was 26 to 44 min. Each of the eight compositions was tested at six water fluxes (11–23 L/m^2/h) and each test was repeated in duplicate (giving a total of $8 \times 6 \times 2 = 96$ tests). After each test, the system was completely flushed by circulating the feed solution for 30 min to ensure that the solution inside the system and feed tank reached a uniform concentration in preparation for the next test (the work exchanger was also drained to remove retained salts from the previous test). Overall, including preliminary tests to debug the system, about 100 h of testing were conducted over a period of one month. Before and after the entire series of tests, a standard performance test was carried out with sodium chloride feed to compare performance and detect any membrane deterioration due to scaling or fouling.

4. Results and discussion

This section first presents the main results in comparison to the results with the NaCl solution. It then compares the performance in standard tests, using NaCl, before and after the whole series of tests with simulated groundwater. To interpret further the findings, the nucleation induction time is compared to the experimental residence times, thus helping to assess the extent to which induction time is a useful predictor of scaling in batch RO. All detailed results from the experiments and the raw experimental data are provided in the supporting information and appended data files.

4.1. Performance comparison: groundwater vs NaCl feed water

4.1.1. Specific energy consumption

Specific energy consumption (SEC) was measured as the total hydraulic work done by the supply and recirculation pumps per m^3 of permeate (i.e., hydraulic *SEC*). The work was calculated as the integral of pressure with volume at the outlet of each pump. For comparison with the NaCl solution, we used solutions of equivalent osmotic pressure. Since all the samples had low concentrations (<5000 mg/L), the osmotic pressures of the simulated groundwater compositions were calculated using the van't Hoff expression, with the help of published osmotic coefficients [42], and were found to be in the range of 1.1 to 3.2 bar [3].

Because the resulting osmotic pressures did not correspond exactly to the concentrations at which the NaCl tests were carried out previously, we used our validated model of the batch RO system to work out the *SEC* values with NaCl. (This model gave hydraulic *SEC* to 3 % accuracy and enabled us to interpolate experimental results based on feed salinity and flux [3]; membrane permeability was adjusted to 4.1 L/m^2/h/bar in the model according to the results of the NaCl performance tests in Section 4.2). Table 6 compares *SEC* at constant flux of 15.6 L/m^2/h. Although groundwater *SEC* was slightly lower than for NaCl, the discrepancy was <7 % (averaging 3.5 %) between the groundwater compositions and pure NaCl solution. This confirmed that tests and models obtained with NaCl were a useful representation of groundwater in all eight cases.

Fig. 3 compares the hydraulic *SEC* measured using the eight groundwater compositions against the NaCl equivalent values at different fluxes. The model predictions agree well with almost all the experimental measurements. Hydraulic pressure caused by hydrodynamic friction in a RO membrane is approximately proportional to the flux ($P \propto J_w/A_w$). Thus, *SEC* increased with water flux because of greater applied pressure by the supply pump – as has previously been reported in both standard and batch RO systems [1,43]. For both Egypt and India compositions, the total hydraulic *SEC* varied from around 0.19 to 0.46 kWh/m^3. The highest *SEC* was measured at the highest tested water flux (J_w ~22.1 L/m^2/h) and the greatest feed concentrations (E4 and I4); whereas the lowest *SEC* was measured at the lowest tested water flux (J_w ~11.4 L/m^2/h) and the lowest feed concentrations (E1 and I1).

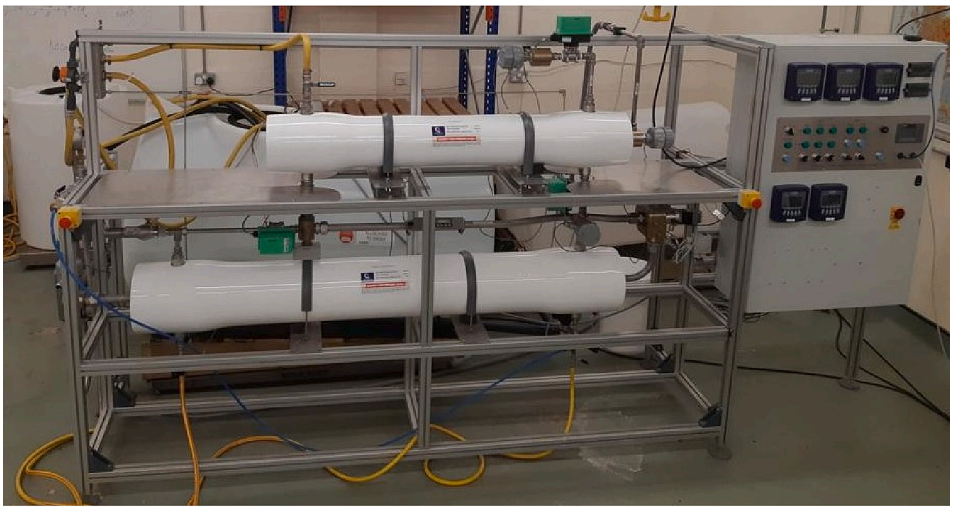

Fig. 2. Photo of the batch RO pilot system at the University of Birmingham.

Table 6
Hydraulic *SEC* with groundwater compared to that with NaCl at equivalent osmotic pressure, at flux J_w ~15.6 L/m^2/h.

	Composition	Osmotic pressure (bar)	Equivalent NaCl concentration (mg/L)	Hydraulic *SEC* (kWh/m^3)		
				Groundwater	NaCl	Error (%)
Egypt	E1	1.12	1420	0.228	0.241	5.4
	E2	1.62	2050	0.286	0.281	1.8
	E3	2.55	3228	0.338	0.352	4
	E4	3.15	3987	0.376	0.398	5.5
India	I1	1.17	1476	0.253	0.253	0.0
	I2	2.11	2673	0.296	0.318	6.9
	I3	2.46	3342	0.351	0.355	1.1
	I4	2.89	3662	0.357	0.383	6.8

Depending on the target specifications, we could choose to achieve higher water output at the cost of higher *SEC*, or lower *SEC* at the cost of less output. For instance, on increasing the water flux from 11.4 to 22.1 L/m^2/h when using sample E4 as the feed solution, the hydraulic *SEC* increased by 37 % while system output rose by 73 % from 9.6 to 16.7 m^3/day (see Fig. 4). Since the *SEC* values are low in all cases, this suggests that a higher water output may be preferred in practice.

4.1.2. Peak pressure

In batch RO, the peak pressure is an important parameter regarding the system design and pressure ratings of the equipment needed; it also limits the final brine concentration achievable. The peak pressures in this study were in the range of 8 to 22 bar, which was within the 25-bar pressure limit of the equipment used. Peak pressure increased with the feed concentration, as shown in Fig. 5. Comparing the peak pressure observed in this study (for both groundwater tests and the performance tests of Section 4.2) against NaCl solutions in [3] at a water flux of approximately 15.6 L/m^2/h revealed similar values, with only minor differences. These differences may be attributed to the membrane's permeability loss, which occurred over a year of membrane use, resulting in a lower water permeation rate of about 4.1 L/m^2/h/bar in this study compared to 4.4 L/m^2/h/bar reported in [3].

4.1.3. Rejection

We also compared the salt rejection results against those in our previous study using NaCl feed (see Fig. 6). In all cases, salt rejection varied between 0.94 and 0.97 with low concentration samples having better salt rejection. This may be due to the lower concentration difference across the membrane [43]. However, it is interesting to note that, the salt rejection was slightly higher with NaCl solution. This may have been due to a drift in membrane properties among the different tests. The higher rejection with NaCl corresponds to a higher differential osmotic pressure which is consistent with the observation of slightly higher *SEC* in Section 4.1.1 above.

4.2. Performance test before and after experiments

Before and after the 100-h series of experiments, we performed a test using a feed solution containing 3000 mg/L of NaCl to determine whether membrane performance had deteriorated. If fouling or scaling occurs at the membrane surface, it will likely cause additional hydraulic resistance and applied pressure will rise, for a fixed water flux and recovery. Fig. 7A shows how pressure changed over the pressurisation phase for the NaCl performance test at $r = 0.8$ and J_w ~22.1 L/m^2/h, comparing the situation before and after the series of experiments. The applied pressure in both tests followed the same pattern with a minor discrepancy (the average pressure values for the performance test before and after trials were 12.44 and 12.36 bar respectively). Fig. 7B also compares the average applied pressure before and after the experiments, as measured by the NaCl performance test at different water fluxes. Surprisingly, a slight decrease (as much as 0.2 bar) in applied pressure was consistently observed. To investigate the possible cause of this decrease, the permeate quality was studied in more detail.

Fig. 8A and B show the conductivity of the RO module inlet and permeate over the pressurisation phase during the NaCl performance tests (at J_w ~22.1 L/m^2/h). Inlet RO conductivity was almost unchanged before and after, with average values of 11.05 and 11.14 mS/cm respectively, i.e., <1 % difference. However, the permeate conductivity after the series of experiments test was slightly increased at 0.29 mS/cm average compared to 0.24 mS/cm before (see Fig. 8B). Similarly, Fig. 8C compares salt rejection at different fluxes showing that rejection deteriorated. This decrease in rejection is consistent with the decrease in

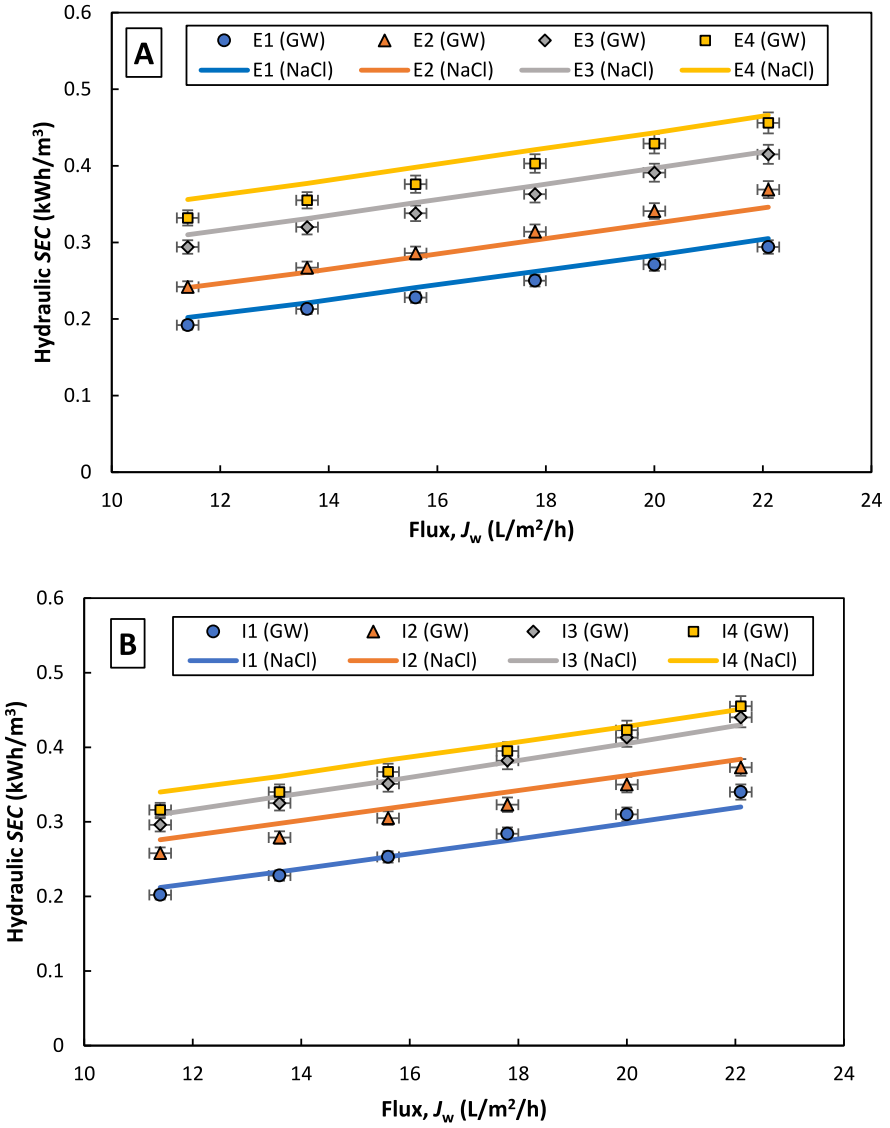

Fig. 3. Total hydraulic *SEC* for A) Egypt and B) India water samples (GW and NaCl represent experimental results for groundwater compositions and modeling values using equivalent NaCl feed respectively) at various water fluxes and $r = 0.8$.

applied pressure, as it corresponds to a slightly decreased osmotic pressure difference across the membrane. This may have been due to some membrane oxidation (despite the use of sodium metabisulphite to neutralise free chlorine) which can cause higher salt passage and loss of rejection. For example, the salt rejection reduced from 0.96 to 0.952 at J_w ~22.1 L/m^2/h after a month of trials.

4.3. Anti-scaling mechanisms

Fig. 9 is a sample of results recorded over two cycles of batch RO operation, showing the flow and conductivity at the inlet to the RO module, and the permeate flow. It illustrates how the four anti-scaling mechanisms occur during each cycle. Each of these mechanisms will next be discussed individually.

4.3.1. Flushing

Flushing in batch RO differs from flushing in standard continuous RO plants as feed water, rather than permeate or clean-in-place chemicals, are used to carry out the flushing. Additionally, since flushing is a necessary step in batch RO to remove the highly concentrated solution from the RO module at the end of the pressurisation phase, it is considerably more frequent than in standard continuous systems, which typically only flush before the startup or during a shutdown.

The flushing volume in each cycle in our experiments was about 16.5 ± 0.3 L, corresponding to the volume of concentrated solution trapped in the RO module ($V_m = A_m{}^*H/2 = 14.6$ L, where A_m and H are membrane area and membrane channel height) plus piping and port dead volumes (about 2 L in total). Relative to the total feed supplied to the system at each cycle, which is 85.5 ± 0.3 L, flushing comprises about 20 % of the total feed supplied in each cycle.

Many studies have confirmed that membrane fouling can be alleviated by flushing [44–48]. However, the membrane flushing process detaches the particles from the membrane surface only, not from the pores. Chen et al. [48] showed 92–100 % water permeability recovery of seawater and brackish water RO membranes fouled with gypsum and calcite when they were flushed with deionized (DI) water. In another study, Chen et al. [46] examined anti-fouling techniques on membranes fouled in pressure retarded osmosis (PRO) process using retentate from a municipal water recycling plant. Without pH correction or antiscalant addition, they observed 85 and 95 % flux recovery using DI water

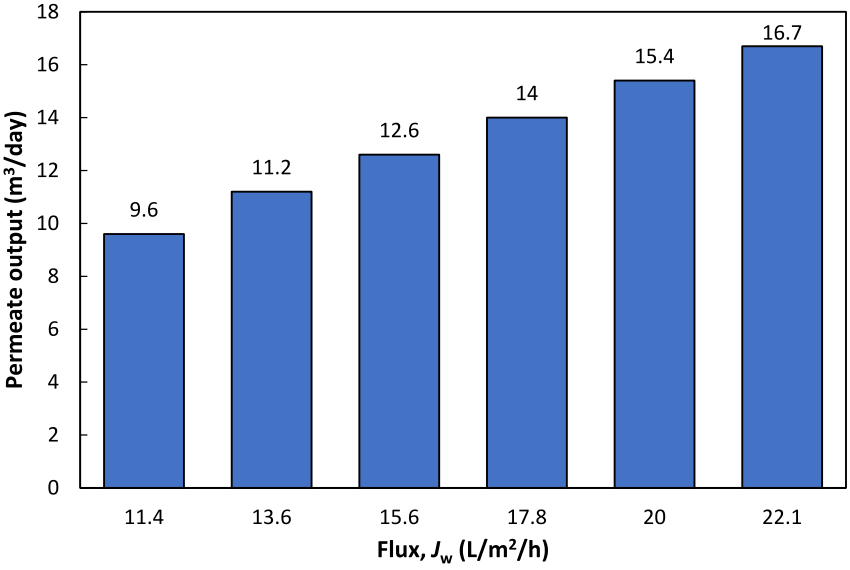

Fig. 4. Total permeate output as a function of water flux using batch RO system, at $r = 0.8$.

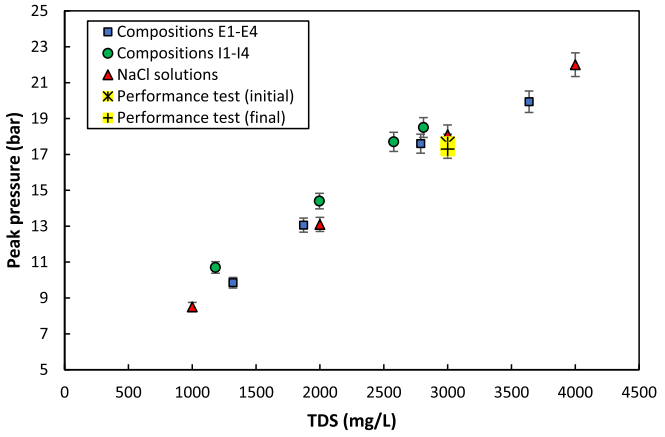

Fig. 5. Comparison of observed peak pressure at various feed samples, simulated groundwater of Egypt (E1-E4) and India (I1-I4) and NaCl solution (1000–4000 mg/L) at $r = 0.8$, and J_w ~15.6 L/m^2/h. Performance tests refer to those described in Section 4.2.

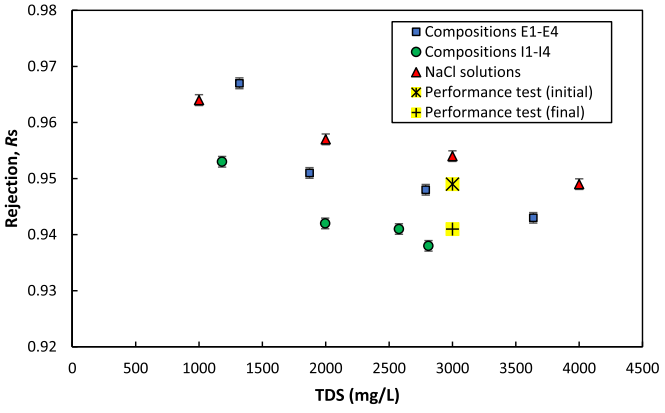

Fig. 6. Comparison of observed salt rejection at various feed samples, simulated groundwater of Egypt (E1-E4) and India (I1-I4) and NaCl solution (1000–4000 mg/L) at $r = 0.8$, and J_w ~15.6 L/m^2/h.

flushing and air bubbling, respectively, under a high cross-flow velocity of 0.23 m/s for 30 min. Flux recovery improved with pH adjustment, reaching 94.6 and 100 % by DI water flushing and air bubbling, respectively. When using antiscalant, flux recovery was almost 100 % with both DI water flushing and air bubbling. De Vries et al. [45] reported the flushing effectiveness on membrane fouling removal using a stop period mechanism. Membranes were flushed at flow velocities of 0.1 and 0.2 m/s at a stop period of 4 min, 24 h, or 4 weeks. They found that longer stop periods improved the fouling removal rate at low feed flow velocities (0.1 m/s), but this effect became less significant at higher flow velocities. It is important to remember, however, that stop periods have the drawback of requiring more membrane surface area to maintain output in compensation for downtime.

In comparison to the studies mentioned, our batch RO system had a much higher frequency of flushing, occurring for 75 s after every 4–8 min of operation at high feed flow velocities (0.8–1.6 m/s). However, in our system, flushing was conducted with feed solution instead of DI water. It is important to note that in the aforementioned studies, flushing was the sole cleaning mechanism, whereas in batch RO a combination of different cleaning mechanisms occurred in the same process. This made it challenging to assess the individual contribution of each mechanism.

4.3.2. *Osmotic backwash*

The amount of osmotic backwash in the batch RO pilot was determined by subtracting the permeate output from the amount of feedwater supplied to the system during the pressurisation phase (see Table 7). Since osmotic backwash is driven by the brine osmotic pressure, which increases with the feed osmotic pressure, we have correlated in Fig. 10 the osmotic backwash volume against feed osmotic pressure, comparing also against experimental values with NaCl solution [3].

Thus, 3.1–4.6 L of osmotic backwash volume in each cycle in our batch RO pilot could be another cause of scaling inhibition. The amount of osmotic backwash was lower than that occurring with pure NaCl solution as feed [3]. This might be because the salt rejection of NaCl solutions was slightly higher than the groundwater compositions; thus, the concentration difference inside the RO module in the case of NaCl solutions was slightly higher and caused more osmotic backwash volume.

Cai et al. [49] reported that, with a membrane fouled by organics, periodic osmotic backwash caused by solar irradiance fluctuation

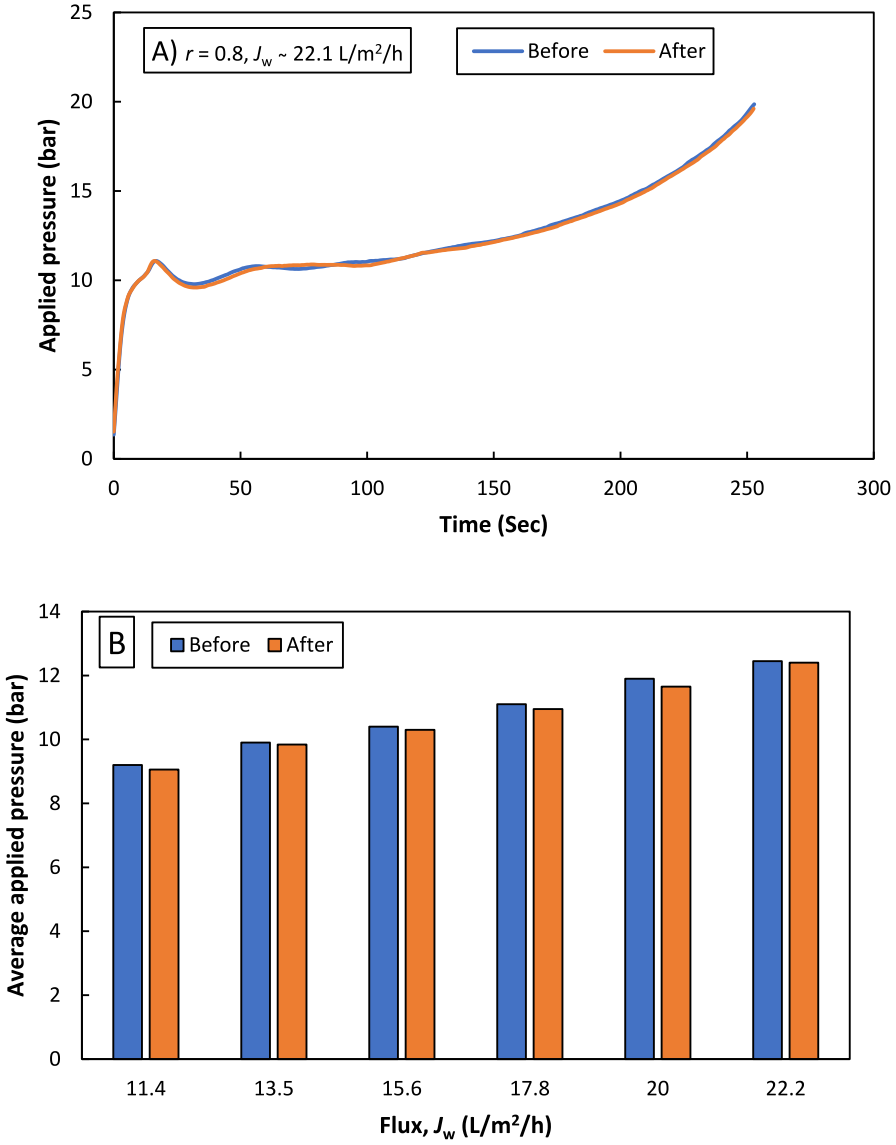

Fig. 7. Performance in NaCl test before and after the simulated groundwater experiments in the batch RO system, A) pressure changes over time in the pressurisation phase and B) Average pressure in the pressurisation phase vs. water flux for a cycle. All the tests were conducted at $r = 0.8$.

restored 46–98 % of the permeate flux, demonstrating the effectiveness of osmotic backwash in reducing membrane fouling. Nevertheless, they observed 2–2.5 $\times$ 10^{-3} L of backwash volume with a membrane active area of 4.7 $\times$ 10^{-3} m^2 compared to the current 3.1–4.6 L backwash volume with the membrane active area of 41 m^2 at almost the same feed osmotic pressure. Expressed per membrane area, Cai et al., therefore used about 0.5 L/m^2 of backwash which compares to only 0.1 L/m^2 in this study, suggesting the contribution in countering fouling may be less in this study. Nonetheless, an increased backwash would decrease system output which is undesirable.

4.3.3. *Feed flow reversal*

In the batch RO system of this study, the flow direction was reversed during the purge phase with feed water replacing the supersaturated solution inside the RO module. The duration of reversed flow was about one fifth that of forward flow in the pressurisation phase. The reversal feed flow velocity ranged from 0.8 to 1.6 m/s and the flow was reversed for a duration of 1.2 min every 4–8 min. It is interesting to compare these parameters against previous studies using non-batch RO systems.

In one such study, Gilron et al. [28] tested a calcium sulfate feed solution with *SI* of 0.54–0.73 and also a calcium carbonate solution with *LSI* of 1.0 at recoveries ranging from 0.67 to 0.82. In the case of calcium sulfate, when applying flow reversal every half hour at recoveries around 0.8, they observed no scaling over the total 18 h of the experiment. In the case of calcium carbonate, when operating at recovery of 0.7 (concentrate *LSI* of 1.5), they observed little sign of scaling when the flow was reversed every hour.

In another previous study, Gu et al. [29] evaluated the technical feasibility and performance of reversal feed flow in a RO pilot system also using calcium sulfate in the feed. Scale detection in an external membrane monitor (MeMo) triggered the reversal of feed flow in their pilot. Scale-free operation was observed while the RO pilot was operated in cyclic reversal flow mode at a recovery of 0.69–0.81 with *SI* reaching 0.54 at the tail element membrane surface. When the pilot was operated without flow reversal at $r = 0.69$, the membrane surface in the MeMo became fully covered by scale in 1.5 h, with 50 % coverage occurring in just 45 min. At the same recovery, and with reversal feed flow triggered when coverage reached 50 %, the 45 min was extended some eight times to 6 h, thus confirming a substantial retardation of scaling.

In summary, the above two studies [28,29] reported significant

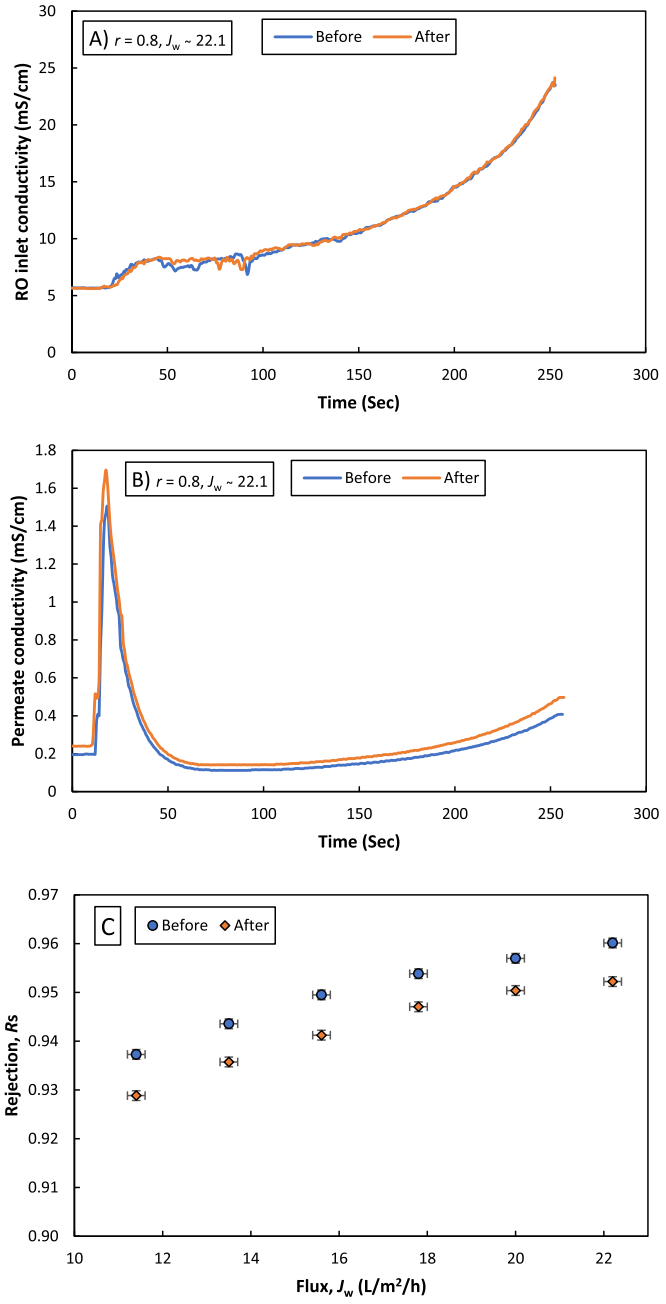

Fig. 8. Results of NaCl performance tests before and after the simulated groundwater experiments, A) RO inlet conductivity variation vs. time over the pressurisation phase, B) permeate conductivity variation vs. time over the pressurisation phase and C) Salt rejection as a function of water flux. All the tests were conducted at $r = 0.8$.

improvements using feed flow reversal that was substantially less frequent than in the current study, i.e., reversing the flow direction only every 30–360 min as opposed to just 4–8 min in the current batch RO experiments. Therefore, it is likely that feed flow reversal has a useful effect in batch RO also.

4.3.4. Salinity cycling

Fig. 11 shows the variation of *LSI* and the corresponding nucleation induction time of calcium carbonate (as calcite) calculated using Eq. (1) over the process time during pressurisation, for compositions I3 and I4 at J_w ~15.6 L/m^2/h and $r = 0.8$. As time passes, the concentration of the solution inside the system increases and consequently the *LSI* also increases, causing the nucleation induction time to decrease. For example, for composition I4, at $r = 0.5$ the *LSI* has risen from the initial value of 1.35 to 1.87 causing the calculated induction nucleation time to drop from 1803 to 59 s. Meanwhile, the process needs to continue for another 135 s to reach the recovery of $r = 0.8$. Thus, severe calcite scaling could be expected to occur before the end of the pressurisation phase. Similar analysis of other tests, corresponding to the other 6 feed compositions, also suggested the risk of scaling due to short nucleation induction time compared to the remaining process time. Nevertheless, such scaling was not evident in our experiments.

Scaling of calcite and gypsum on RO membrane occurs through two routes: bulk deposition or homogenous nucleation, and surface crystallization or heterogeneous nucleation. In general, the time required in heterogenous crystalization (on the membrane surfaces and in the presence of the seeds) is significantly shorter compared to the crystallization induction time in solutions which is the basis for Eqs. (1) and (2) [50]. Thus, scaling might be expected to occur even earlier than indicated in Fig. 11.

Purging at each salinity cycle of the batch RO could be more effective at the initial stage of the formation of crystals since they are smaller and may be removed with a shorter purging interval. Surface crystals can become larger with each cycle if they are not entirely removed, which could make purging less effective than anticipated. Therefore, it would be desirable to completely remove any crystals and nuclei that may have developed on the membrane surface during the water production phase.

Over the purging period, the brine salinity and saturation indices both drop to below saturation. After each filtration phase, which took about 250–500 s in the batch RO pilot in this study, flow was reversed during the purging phase for about 75 s. As a result, the saturation index could be consistently reset at the end of the purge phase to the values slightly higher than the initial values of the feed solution (due to the salt retention).

4.4. Future work

Regarding further work, although the current study showed that batch RO can maintain performance even without the use of anti-scalant chemicals, it will be worth investigating performance when an anti-scalant is used. Batch RO may decrease the anti-scalant dosage needed with highly supersaturated feed solutions and high recoveries, reducing the operational cost and environmental impact of dosing anti-scalants. It would also be interesting to carry tests with salts such as calcium phosphate against which anti-scalants have been shown to be ineffective in conventional RO [51].

Another critical consideration is whether this concept can be successfully applied to scaled-up systems using more than one RO element. A system can be scaled up either by adding elements in series, in parallel, or a combination of series and parallel. Parallel configurations are expected to behave the same as the 1-element system as the flow conditions in each element will be unchanged. However, it would be costly to scale up using a parallel-only configuration because of the large number of vessels, end caps, and piping connections [52]. Use of elements in series is therefore desirable. Considering the presence of the four mechanisms of scaling mitigation in batch RO, we are of the opinion systems using 2–4 elements [32] would indeed continue to exhibit resistance to fouling. However, to confirm whether the behaviour of a multi-module batch RO system aligns with that of a single module, further studies are necessary.

Based on the findings presented in our previous studies [1,3], it was determined that, for low concentrations (<5000 mg/L) and low applied pressures (<25 bar), the optimal recirculation to feed flow ratio is approximately 2 to minimize the overall *SEC*. This corresponds to a recovery per pass of approximately 0.33 which is somewhat higher than the typical range of 0.12–0.2 used in industrial standard RO systems [53]. In future research, it would be intriguing to expand the study to encompass higher recirculation flows along with more challenging

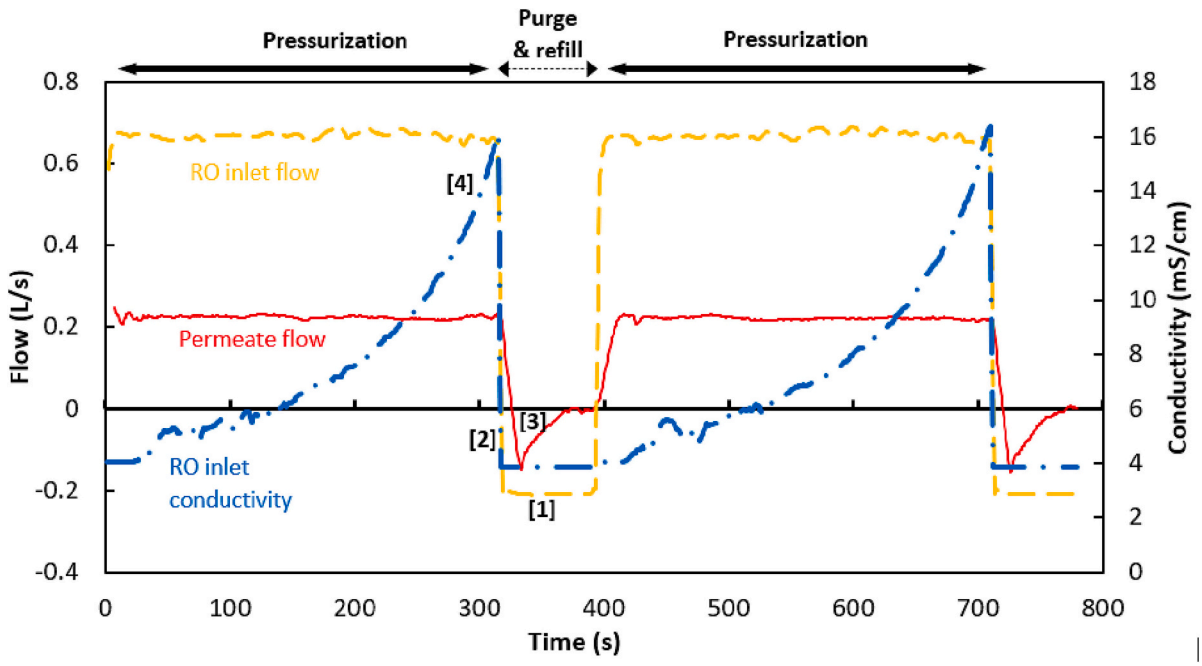

Fig. 9. Mechanisms of scaling inhibition in the batch RO cycle: [1] periodic flushing occurs during each purge-and-refill phase: permeate output pauses while tangential flow over the membrane (represented by RO inlet flow) continues at low salinity (represented by conductivity); [2] flow reversal, shown as a negative RO inlet flow, during purge-and-refill; [3] osmotic backwash, evident as a negative permeate flow; [4] salinity cycling evident from the saw tooth pattern of conductivity at the RO inlet. Data measured with composition E2 at J_w ~17.8 L/m^2/h. Note: The permeate flow was measured as the rate of decrease of the sum of feed and brine tank weights. A decrease in this sum indicates an outflow via the permeate, whereas an increase indicates the osmotic backwash. A moving average trendline was used to smooth the data.

Table 7
Permeate and osmotic backwash volume in every batch cycle (69 L) for all the compositions tested.

Composition	TDS (mg/L)	Permeate volume (L)	Osmotic backwash volume (L)
E1	1319	65.4	3.6
E2	1871	65.3	3.7
E3	2788	64.6	4.4
E4	3637	64.4	4.6
I1	1180	65.9	3.1
I2	1994	65.0	4.0
I3	2576	64.7	4.3
I4	2811	64.6	4.4

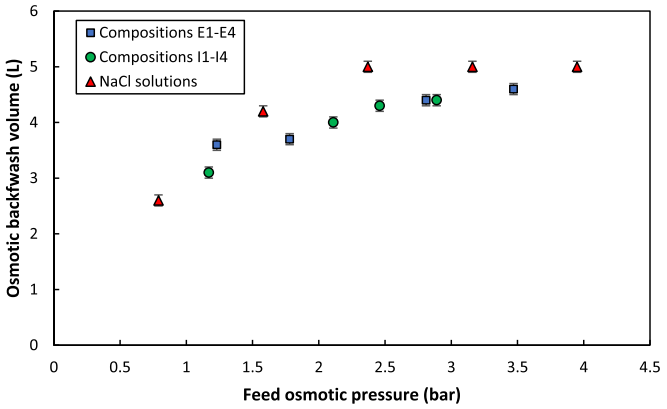

Fig. 10. Osmotic backwash volume vs. osmotic feed pressure, for groundwater compositions and pure NaCl feed solution at recovery $r = 0.8$.

fouling feed compositions. By employing larger ratios, the concentration polarization can be reduced, which may offer advantages in terms of fouling prevention. *SEC* would increase slightly but, based on previous studies, the penalty in increasing the flow ratio from 2 to say 3 would only be about 4 % [3].

This study has focused on desalination of groundwater containing high levels of sparingly soluble salts that may cause scaling. However, in RO processes, there are various other types of fouling that can be encountered, including particulate fouling, organic fouling, and biofouling, all of which are important for future research. For instance, natural water often contains a certain level of silica, causing colloidal fouling which is often challenging to control [54]. Additionally, apart from scaling (which usually starts in the tail element) other forms of fouling commonly occur in the lead element [55]. Among the fouling removal methods mentioned in Section 4.3, osmotic backwash is thought to have the highest potential for minimizing or preventing these types of fouling. Nevertheless, conducting future studies that consider each type of fouling would greatly contribute to a better understanding of the potential of batch RO in fouling minimization. Moreover, studies have shown interactions among the various foulants [56] such that studies of combined (and not just individual) foulants will also be important.

Overall, conducting long-term pilot testing using ample sources of real feed water that have a high likelihood of experiencing various forms of fouling in the field is imperative to comprehensively evaluate the system. This approach will allow for a thorough assessment of the impact of the aforementioned fouling mitigation mechanisms in batch RO and a comparison against standard continuous RO systems. Such testing will provide valuable insights into the system's performance and effectiveness in real-world scenarios and help evaluate its practical viability and reliability.

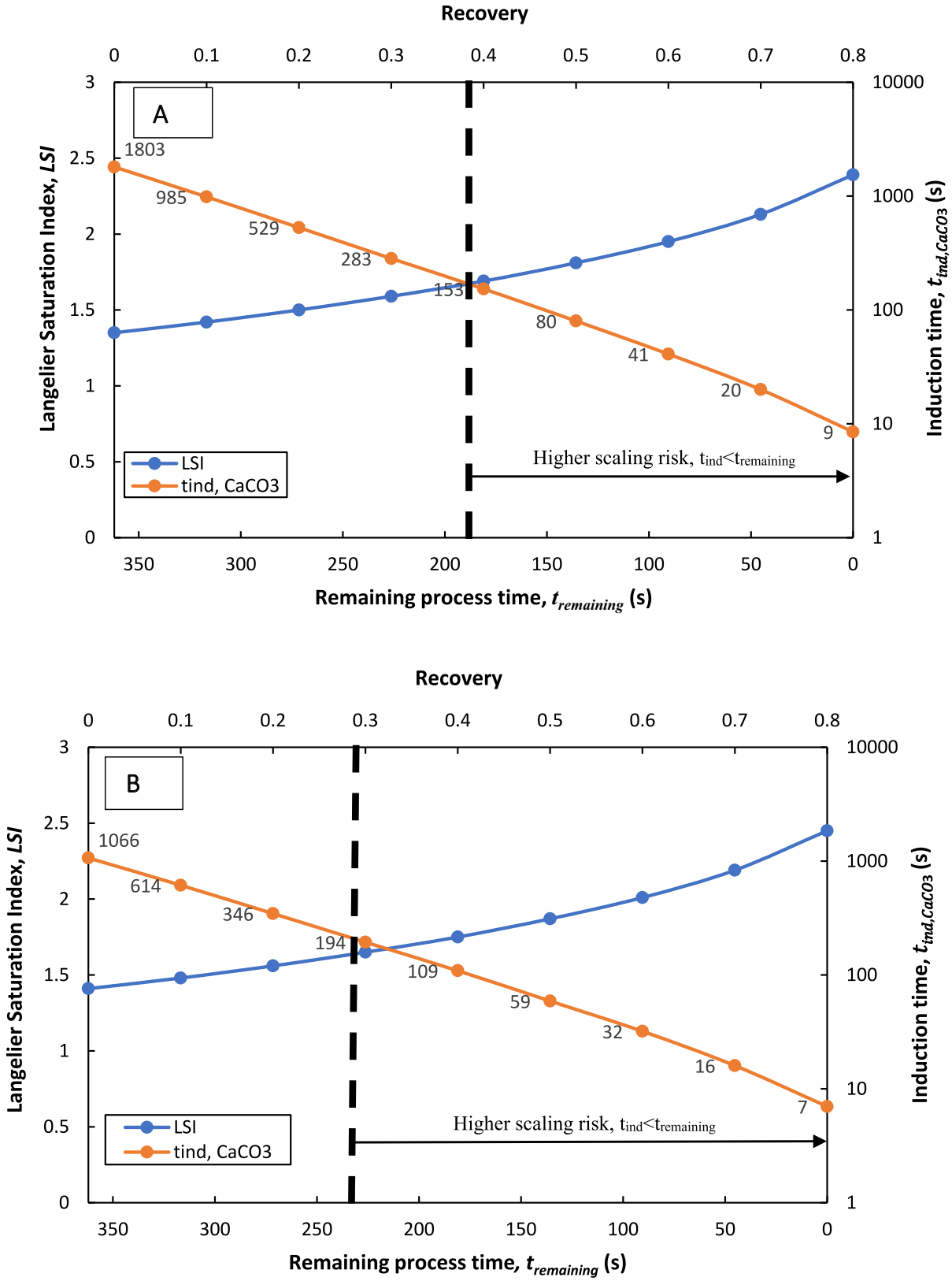

Fig. 11. Progress of Langelier saturation index and corresponding nucleation induction time for $CaCO_3$ (as calcite) as a function of remaining process time and recovery at J_w ~15.6 L/m^2/h. A) composition I3, and B) composition I4. The vertical dashed line indicates the threshold where the calculated induction time becomes less than the remaining process time ($t_{ind} < t_{remaining}$), indicating the risk of scaling.

5. Conclusion

An experimental investigation has been undertaken in a free-piston batch RO pilot to compare the performance in treating brackish groundwater at high recovery ($r = 0.8$) against the performance of the same system treating pure NaCl solution. Eight feedwater compositions were replicated in the lab, using field data taken from two locations (one in Egypt and one in India) where raw groundwater quality is not acceptable. The *SEC* of the system was within 7 % of that obtained with NaCl solutions having equivalent osmotic pressure. This confirmed that studies conducted with pure NaCl solutions are a reasonable representation of the more complex salt mixtures in the groundwater.

The saturation level of sparingly soluble salts suggested a significant risk of calcite ($CaCO_3$) and fluorite (CaF_2) scaling at the RO outlet. Nonetheless, over the duration of these tests (totalling >100 h), the batch RO system resisted scaling. This was confirmed by two performance tests with a 3000 mg/L NaCl feed solution, conducted before and after the entire test series. No increase in transmembrane pressure was observed. Absence of scaling is attributed to mechanisms of periodic flushing, flow reversal, osmotic backwash, and salinity cycling. Flushing occurred during 15–20 % of the operation time, after the end of each pressurisation phase, in the reverse direction to the feed flow during pressurisation. Osmotic backwash of 3.1–4.6 L occurred (a similar amount to that observed with pure NaCl feed). A careful study of the saturation and expected nucleation induction for crystallization of calcite and gypsum during each batch RO cycle showed that, in all the tests conducted, there was theoretically sufficient time for crystallization to begin. Nevertheless, no deterioration in performance was observed suggesting that no crystallization and scaling occurred. Comparisons against the literature suggest that the other three mechanisms (i.e., flushing, osmotic backwash, and flow reversal) were also likely contributors to scaling inhibition.

CRediT authorship contribution statement

Ebrahim Hossseinipour: Writing – original draft, Investigation, Conceptualization. **Ellie Harris:** Investigation. **Hossam A. El Nazer:** Writing – review & editing, Funding acquisition. **Yasser M.A. Mohamed:** Writing – review & editing. **Philip A. Davies:** Conceptualization, Writing – review & editing, Supervision, Project administration, Funding acquisition.

Declaration of competing interest

The authors would like to declare that a spinout company (Salinity Solutions Ltd.) was formed to exploit the batch RO technology, and that one of the authors (PAD) has an equity stake in this company.

Data availability

Shared data are included as files in the supporting material

Acknowledgements

The authors acknowledge funding from the British Council Newton Fund Institutional Links programme (STDF project ID:42703) and the Engineering and Physical Sciences Research Council (Grant Ref: EP/T025867/1). The authors thank the National Research Center (Egypt) for its valuable support. They also thank Paris Pasqualin for his comments on the manuscript.

Appendix A

Table A1
Reported analyses of samples on which feed compositions are based. Ion concentrations below 1 mg/L are neglected.

	Composition	Sample[a]	pH	TDS (mg/L)	EC (μS/cm)	Ca^{2+} (mg/L)	Mg^{2+} (mg/L)	Na^{+} (mg/L)	K^{+} (mg/L)	NH_4^{+} (mg/L)	HCO_3^{-} (mg/L)	Cl^{-} (mg/L)	SO_4^{2-} (mg/L)	NO_3^{-} (mg/L)
Egypt	E1	SN52	7.5	1367	2229	80	38.4	316.5	9.4	0.3	136.6	462	276.5	0.8
	E2	SN11	7.3	1853	2793	128	62.4	423.2	20.3	0.4	131.8	700	401.3	1.5
	E3	SN29	7.3	2961	4540	152	115.2	671.6	25.9	0.6	170.8	1288	358.3	2.1
	E4	SN33	7.2	3492	5149	224	81.6	955.0	28.4	0.7	119.6	1554	666.6	1.9
India	I1	LG14	6.3	1138	1897	196	2.4	138	4	–	310	400	80	94
	I2	LG13	6.3	2090	3490	304	69.6	200	5	–	305	975	98	106
	13	LG12	6.3	2600	4330	412	52.8	408	11	–	305	1225	133	26
	I4	LG2	6.5	3080	5130	492	28.8	426	31	–	305	1400	113	52

[a] Sample numbering as used in source references [37, 38].

Appendix B. Supplementary data

Supplementary data to this article can be found online at https://doi.org/10.1016/j.desal.2023.116875.

References

[1] E. Hosseinipour, S. Karimi, S. Barbe, K. Park, P.A. Davies, Hybrid semi-batch/batch reverse osmosis (HSBRO) for use in zero liquid discharge (ZLD) applications, Desalination 544 (2022), 116126.
[2] Q.J. Wei, C.I. Tucker, P.J. Wu, A.M. Trueworthy, E.W. Tow, J.H. Lienhard, Impact of salt retention on true batch reverse osmosis energy consumption: experiments and model validation, Desalination 479 (2020), 114177.
[3] E. Hosseinipour, K. Park, L. Burlace, T. Naughton, P.A. Davies, A free-piston batch reverse osmosis (RO) system for brackish water desalination: experimental study and model validation, Desalination 527 (2022), 115524.
[4] E. Jones, M. Qadir, M.T. van Vliet, V. Smakhtin, S.-M. Kang, The state of desalination and brine production: a global outlook, Sci. Total Environ. 657 (2019) 1343–1356.
[5] J.W. Delleur, The Handbook of Groundwater Engineering, CRC press, 2006.
[6] Q. Liu, G.-R. Xu, R. Das, Inorganic scaling in reverse osmosis (RO) desalination: mechanisms, monitoring, and inhibition strategies, Desalination 468 (2019), 114065.
[7] S. Oren, L. Birnhack, O. Lehmann, O. Lahav, A different approach for brackish-water desalination, comprising acidification of the feed-water and CO2 (aq) reuse for alkalinity, Ca2+ and Mg2+ supply in the post treatment stage, Sep. Purif. Technol. 89 (2012) 252–260.
[8] S. Shirazi, C.-J. Lin, D. Chen, Inorganic fouling of pressure-driven membrane processes—a critical review, Desalination 250 (2010) 236–248.
[9] J. Benecke, J. Rozova, M. Ernst, Anti-scale effects of select organic macromolecules on gypsum bulk and surface crystallization during reverse osmosis desalination, Sep. Purif. Technol. 198 (2018) 68–78.
[10] C. Fritzmann, J. Löwenberg, T. Wintgens, T. Melin, State-of-the-art of reverse osmosis desalination, Desalination 216 (2007) 1–76.
[11] X. Xu, J.E. Ness, A. Miara, K.A. Sitterley, M. Talmadge, B. O'Neill, K. Coughlin, S. Akar, E.T. Edirisooriya, P. Kurup, Analysis of brackish water desalination for

municipal uses: case studies on challenges and opportunities, ACS ES&T Engineering 2 (2022) 306–322.
[12] A. Ruiz-García, I. Nuez, M. Carrascosa-Chisvert, J. Santana, Simulations of BWRO systems under different feedwater characteristics. Analysis of operation windows and optimal operating points, Desalination 491 (2020), 114582.
[13] A. Matin, F. Rahman, H.Z. Shafi, S.M. Zubair, Scaling of reverse osmosis membranes used in water desalination: phenomena, impact, and control; future directions, Desalination 455 (2019) 135–157.
[14] A. Ruiz-García, J. Feo-García, Antiscalant cost and maximum water recovery in reverse osmosis for different inorganic composition of groundwater, Desalin. Water Treat. 73 (2017) 46–53.
[15] L. Burlace, P. Davies, Fouling and fouling mitigation in batch reverse osmosis: review and outlook, Desalin. Water Treat. 249 (2022) 1–22.
[16] A. Matin, T. Laoui, W. Falath, M. Farooque, Fouling control in reverse osmosis for water desalination & reuse: current practices & emerging environment-friendly technologies, Sci. Total Environ. 765 (2021), 142721.
[17] J.-J. Qin, M.H. Oo, K.A. Kekre, B. Liberman, Development of novel backwash cleaning technique for reverse osmosis in reclamation of secondary effluent, J. Membr. Sci. 346 (2010) 8–14.
[18] E. Bar-Zeev, M. Elimelech, Reverse osmosis biofilm dispersal by osmotic back-flushing: cleaning via substratum perforation, Environmental Science & Technology Letters 1 (2014) 162–166.
[19] J. Park, W. Jeong, J. Nam, J. Kim, J. Kim, K. Chon, E. Lee, H. Kim, A. Jang, An analysis of the effects of osmotic backwashing on the seawater reverse osmosis process, Environ. Technol. 35 (2014) 1455–1461.
[20] W. Jiang, Y. Wei, X. Gao, C. Gao, Y. Wang, An innovative backwash cleaning technique for NF membrane in groundwater desalination: fouling reversibility and cleaning without chemical detergent, Desalination 359 (2015) 26–36.
[21] J.W. Nam, J.Y. Park, J.H. Kim, Y.S. Lee, E.J. Lee, M.J. Jeon, H.S. Kim, A. Jang, Effect on backwash cleaning efficiency with TDS concentrations of circulated water and backwashing water in SWRO membrane, Desalin. Water Treat. 43 (2012) 124–130.
[22] E.W. Tow, M.M. Rencken, In situ visualization of organic fouling and cleaning mechanisms in reverse osmosis and forward osmosis, Desalination 399 (2016) 138–147.
[23] S. Daly, A. Allen, V. Koutsos, A.J. Semião, Influence of organic fouling layer characteristics and osmotic backwashing conditions on cleaning efficiency of RO membranes, J. Membr. Sci. 616 (2020), 118604.
[24] Y.-A. Boussouga, B.S. Richards, A.I. Schäfer, Renewable energy powered membrane technology: system resilience under solar irradiance fluctuations during the treatment of fluoride-rich natural waters by different nanofiltration/reverse osmosis membranes, J. Membr. Sci. 617 (2021), 118452.
[25] M.N. Mangal, S.G. Salinas-Rodriguez, J. Dusseldorp, B. Blankert, V.A. Yangali-Quintanilla, A.J. Kemperman, J.C. Schippers, W.G. van der Meer, M.D. Kennedy, Foulant identification and performance evaluation of antiscalants in increasing the recovery of a reverse osmosis system treating anaerobic groundwater, Membranes 12 (2022) 290.
[26] L. Fortunato, A.H. Alshahri, A.S. Farinha, I. Zakzouk, S. Jeong, T. Leiknes, Fouling investigation of a full-scale seawater reverse osmosis desalination (SWRO) plant on the Red Sea: membrane autopsy and pretreatment efficiency, Desalination 496 (2020), 114536.
[27] M. Li, N. Chan, J. Li, Novel dynamic and cyclic designs for ultra-high recovery waste and brackish water RO desalination, Chem. Eng. Res. Des. 179 (2022) 473–483.
[28] J. Gilron, M. Waisman, N. Daltrophe, N. Pomerantz, M. Milman, I. Ladizhansky, E. Korin, Prevention of precipitation fouling in NF/RO by reverse flow operation, Desalination 199 (2006) 29–30.
[29] H. Gu, A.R. Bartman, M. Uchymiak, P.D. Christofides, Y. Cohen, Self-adaptive feed flow reversal operation of reverse osmosis desalination, Desalination 308 (2013) 63–72.
[30] S. Cordoba, A. Das, J. Leon, J.M. Garcia, D.M. Warsinger, Double-acting batch reverse osmosis configuration for best-in-class efficiency and low downtime, Desalination 506 (2021), 114959.
[31] P. Davies, A. Afifi, F. Khatoon, G. Kuldip, S. Javed, S. Khan, Double-acting batch-RO system for desalination of brackish water with high efficiency and high recovery, in: Desalination for the Environment–Clean Energy and Water, Rome, 2016, pp. 23–25.
[32] H. Abu Ali, M. Baronian, L. Burlace, P.A. Davies, S. Halasah, M. Hind, A. Hossain, C. Lipchin, A. Majali, M. Mark, Off-grid desalination for irrigation in the Jordan Valley, Desalin. Water Treat. 168 (2019) 143–154.
[33] D.M. Warsinger, E.W. Tow, L.A. Maswadeh, G.B. Connors, J. Swaminathan, J. H. Lienhard, Inorganic fouling mitigation by salinity cycling in batch reverse osmosis, Water Res. 137 (2018) 384–394.
[34] M. Li, Cyclic simulation and energy assessment of closed-circuit RO (CCRO) of brackish water, Desalination 545 (2023), 116149.
[35] M. El Hossary, Evaluation and management of groundwater resources in Siwa area with emphasis on the Nubia Sandstone aquifer, Geology Department 138 (1999).
[36] S. Salman, E.A. El Ella, E. Seleem, A. Elnazer, Groundwater quality and environmental investigations in Siwa Oasis, Egypt, International Journal of Recent Advances in Multidisciplinary Research 5 (2018) 3951–3958.
[37] A.A. Elnazer, S.A. Salman, Y. Mohamed, J. Stafford, P. Davies, H.A. El Nazer, Siwa Oasis groundwater quality: factors controlling spatial and temporal changes, Environ. Monit. Assess. 195 (2023) 1–14.
[38] R.P. Pujari, N. Labhsetwar, G.C. Quesada, C.Y. Lopez, Deliverable 5.2 of the EU H2020 project bio-mimetic and photo technologies designed for low-cost purification and recycling of water, in: Geo-hydrological Ecological Status of Microwatersheds, 2020 in, https://cordis.europa.eu/project/id/820906/results.
[39] D.L. Parkhurst, C. Appelo, Description of input and examples for PHREEQC version 3—a computer program for speciation, batch-reaction, one-dimensional transport, and inverse geochemical calculations, US Geological Survey Techniques and Methods 6 (2013) 497.
[40] N. AlSawaftah, W. Abuwatfa, N. Darwish, G. Husseini, A comprehensive review on membrane fouling: mathematical modelling, prediction, diagnosis, and mitigation, Water 13 (2021) 1327.
[41] E. Smith, W. Davison, J. Hamilton-Taylor, Methods for preparing synthetic freshwaters, Water Res. 36 (2002) 1286–1296.
[42] R.A. Robinson, R.H. Stokes, Electrolyte Solutions, Courier Corporation, 2002.
[43] L. Wang, T. Cao, J.E. Dykstra, S. Porada, P. Biesheuvel, M. Elimelech, Salt and water transport in reverse osmosis membranes: beyond the solution-diffusion model, Environ. Sci. Technol. 55 (2021) 16665–16675.
[44] J. Zhang, K. Northcott, M. Duke, P. Scales, S.R. Gray, Influence of pre-treatment combinations on RO membrane fouling, Desalination 393 (2016) 120–126.
[45] H.J. de Vries, E. Kleibusch, G.D. Hermes, P. van den Brink, C.M. Plugge, Biofouling control: the impact of biofilm dispersal and membrane flushing, Water Res. 198 (2021), 117163.
[46] S.C. Chen, G.L. Amy, T.-S. Chung, Membrane fouling and anti-fouling strategies using RO retentate from a municipal water recycling plant as the feed for osmotic power generation, Water Res. 88 (2016) 144–155.
[47] G.Z. Ramon, T.-V. Nguyen, E.M. Hoek, Osmosis-assisted cleaning of organic-fouled seawater RO membranes, Chem. Eng. J. 218 (2013) 173–182.
[48] Y. Chen, Y. Cohen, Calcium sulfate and calcium carbonate scaling of thin-film composite polyamide reverse osmosis membranes with surface-tethered polyacrylic acid chains, Membranes 12 (2022) 1287.
[49] Y.-H. Cai, C.J. Burkhardt, A.I. Schäfer, Renewable energy powered membrane technology: impact of osmotic backwash on organic fouling during solar irradiance fluctuation, J. Membr. Sci. 647 (2022), 120286.
[50] T. Lee, J.Y. Choi, Y. Cohen, Gypsum scaling propensity in semi-batch RO (SBRO) and steady-state RO with partial recycle (SSRO-PR), J. Membr. Sci. 588 (2019), 117106.
[51] M.N. Mangal, S.G. Salinas-Rodriguez, J. Dusseldorp, A.J. Kemperman, J. C. Schippers, M.D. Kennedy, W.G. van der Meer, Effectiveness of antiscalants in preventing calcium phosphate scaling in reverse osmosis applications, J. Membr. Sci. 623 (2021), 119090.
[52] H. Kotb, E. Amer, K. Ibrahim, On the optimization of RO (reverse osmosis) system arrangements and their operating conditions, Energy 103 (2016) 127–150.
[53] FilmTec DuPont, Reverse Osmosis Membranes Technical Manual, in, DuPont Wilmington, DE, USA, 2020.
[54] Y.-M. Park, K.-M. Yeon, C.-H. Park, Silica treatment technologies in reverse osmosis for industrial desalination: a review, Environmental Engineering Research 25 (2020) 819–829.
[55] W. Jiang, X. Xu, L. Lin, H. Wang, R. Shaw, D. Lucero, P. Xu, A pilot study of an electromagnetic field for control of reverse osmosis membrane fouling and scaling during brackish groundwater desalination, Water 11 (2019) 1015.
[56] A. Karanasiou, A. Karabelas, S. Mitrouli, Incipient membrane scaling in the presence of polysaccharides during reverse osmosis desalination in spacer-filled channels, Desalination 500 (2021), 114821.